catalysts

MDPI

Article

Bio-Fabrication of Cu/Ag/Zn Nanoparticles and Their Antioxidant and Dye Degradation Activities

Srijal Kunwar [1], Arpita Roy [1,*], Utsav Bhusal [1], Amel Gacem [2], Mahmood M. S. Abdullah [3], Promila Sharma [4], Krishna Kumar Yadav [5,6], Sarvesh Rustagi [7], Nidhi Chatterjee [8], Vishal Kumar Deshwal [8], Hyun-Kyung Park [9] and Byong-Hun Jeon [10,*]

1 Department of Biotechnology, Sharda School of Engineering & Technology, Sharda University, Greater Noida 201310, India; 2019004324.srijal@ug.sharda.ac.in (S.K.); 2019006613.utsav@ug.sharda.ac.in (U.B.)
2 Department of Physics, Faculty of Sciences, University 20 Août 1955, Skikda 21000, Algeria; gacem_amel@yahoo.fr
3 Department of Chemistry, College of Science, King Saud University, P.O. Box 2455, Riyadh 11451, Saudi Arabia; maltaiar@ksu.edu.sa
4 Department of Life Sciences, Graphic Era Deemed to Be University, Dehradun 248002, Uttarakhand, India; promilasharma.bt@geu.ac.in
5 Faculty of Science and Technology, Madhyanchal Professional University, Ratibad, Bhopal 462044, India; envirokrishna@gmail.com
6 Environmental and Atmospheric Sciences Research Group, Scientific Research Center, Al-Ayen University, Thi-Qar, Nasiriyah 64001, Iraq
7 School of Applied and Life Sciences, Uttaranchal University Dehradun, Dehradun 248007, Uttarakhand, India; sarveshrustagi@gmail.com
8 Department of Life Science, Guru Nanak College of Pharmaceutical Sciences, Dehradun 248007, India; nidheechatterjee@gmail.com (N.C.); vishal@bfitdoon.com (V.K.D.)
9 Department of Pediatrics, Hanyang University College of Medicine, 222 Wangsimni-ro, Seongdong-gu, Seoul 04763, Republic of Korea; neopark@hanyang.ac.kr
10 Department of Earth Resources & Environmental Engineering, Hanyang University, 222-Wangsimni-ro, Seongdong-gu, Seoul 04763, Republic of Korea
* Correspondence: arbt2014@gmail.com (A.R.); bhjeon@hanyang.ac.kr (B.-H.J.)

Abstract: The biological synthesis of nanoparticles with copper, silver, and zinc (Cu, Ag, Zn) is reported in this study, adopting a greener, safe, reliable, and eco-friendly approach by using an aqueous leaf extract of *Catharanthus roseus*. The synthesised trimetallic nanoparticles were characterised using different characterisation techniques. The UV–visible spectroscopic technique was initially used to assess nanoparticle formation, in which absorption bands were observed at 220, 270, and 370 nm for Cu, Zn, and Ag nanocomposites, respectively. XRD revealed that the average crystalline size of the nanocomposites was 34.67 nm. The roles of reducing and capping/stabilising agents in the synthesis of Cu/Ag/Zn nanoparticles were confirmed by FTIR analysis, and the successful biosynthesis of the same was also confirmed by X-ray energy-dispersive spectroscopy (EDX) analysis. Potential applications of these synthesised trimetallic nanoparticles were evaluated by assessing their antioxidant and catalytic dye degradation activities. The antioxidant activity of the synthesised nanomaterial was studied using the DPPH assay. The catalytic breakdown of the harmful dyes phenol red and eosin yellow was examined using $NaBH_4$ as a reducing agent. The results showed that the nanomaterial's radical scavenging capacity at 1000 ug/mL was 75.76% and the degradation of these dyes was up to 78% in the presence of $NaBH_4$. Furthermore, the biogenic trimetallic nanomaterial exhibited effective catalytic degradation activity against methyl red and phenol red dyes.

Keywords: *Catharanthus roseus*; trimetallic nanoparticles; catalytic dye degradation; antioxidant activity; green synthesis

Citation: Kunwar, S.; Roy, A.; Bhusal, U.; Gacem, A.; Abdullah, M.M.S.; Sharma, P.; Yadav, K.K.; Rustagi, S.; Chatterjee, N.; Deshwal, V.K.; et al. Bio-Fabrication of Cu/Ag/Zn Nanoparticles and Their Antioxidant and Dye Degradation Activities. *Catalysts* **2023**, *13*, 891. https://doi.org/10.3390/catal13050891

Academic Editors: Pritam Kumar Dikshit and Beom Soo Kim

Received: 26 April 2023
Revised: 9 May 2023
Accepted: 12 May 2023
Published: 15 May 2023

1. Introduction

Over the last few decades, nanotechnology has become a field of extensive research due to its wide applications for human benefit, including medical science, as nanoclusters have a distinct size of less than 100 nm and possess a high surface area. This field of science has the potential to generate a more secure, clean, and useful living environment by using relatively greener nanotechnologies than remediation by industrial chemicals and dangerous contaminants. The idea of green nanotechnology has been explored to develop environmentally friendly processes for the synthesis of nanoparticles. Various categories of nanoparticles have been identified, including organic and inorganic nanoparticles. Of these, metal nanoparticles have attracted a great deal of attention from researchers because of their remarkable physical, chemical, optical, and magnetic characteristics. These distinctive properties of metal nanoparticles are closely associated with their size and shape [1]. Chemical or physical methods are routinely used to synthesise these different metal nanoparticles, including monometallic, bimetallic, and trimetallic NPs. The most commonly used chemical and physical synthesis methods of nanoparticles include the sol-gel method [2], vapour-phase method [3], pulsed laser deposition [4], atomic-layer deposition [5], micro-emulsion [6], laser ablation [7], and pyrolysis [8]. However, the need for biological methods is increasing due to the fact that the traditional methods of isolating nanoparticles are expensive, time-consuming, hazardous, and labour-intensive [9]. For the biosynthesis of nanoparticles, microorganisms (such as bacteria, fungi, yeasts, and algae) and plants are two peculiar biogenic sources that have the potential to be used as bioreducing agents, as the selection of green resources for solvents, reducing agents, and stabilising/capacitation agents are three major criteria that must be carefully considered in the green synthesis strategy [10]. Plants have been considered to be one of the most promising sources of green synthesis since an environmentally benign path can be taken for nanoparticle (NP) biosynthesis [11]. The fabrication of NPs using green methods as an easy, reliable, environmentally acceptable, and economically advantageous substitute for harmful chemicals typically used as reducing or capping agents is one of the main goals of green synthesis techniques [12].

Metal NPs are classified as monometallic (single metal), bimetallic (two metals), or trimetallic NPs based on the number of metals/metal oxides involved. In comparison to mono- and bimetallic nanomaterials, trimetallic NPs have recently gained interest due to their exceptional features, strong qualities, and enhanced physiochemical properties; for example, their physical, chemical, optical, and magnetic properties due to the combined synergistic effects of their metal counterparts [13]. Different electrochemical synthesis methods have been extensively used in practice for the fabrication of trimetallic nanoparticles, whereas only a few reports have been made to date utilising green synthesis techniques. The monometallic nanoparticle biosynthesis method is quite popular. Although some green methods use various techniques, such as microwave irradiation [14] and electrophoretic decomposition [15], some use various parts of plant organs, such as flowers [16], leaves [17], and so on, as reducing agents to reduce metal ions and create the corresponding metal or metal oxide NPs.

Catharanthus roseus is a dicotyledonous angiosperm belonging to the family Apocynaceae and has medicinal properties. The name of the plant known as Madagascar periwinkle or *Catharanthus*, originates from Greek and signifies "pure flower." Meanwhile, the term *Roseus* means the shades red, rose, or pink. Although native and restricted to Madagascar, this plant is also cultivated as an ornamental and medicinal plant in other locations. The plant contains more than 400 alkaloids, including vinblastine, vincristine, tabersonine, vindesine, actineoplastidemeric, etc. Cinchonium oxide is mostly found in the aerial parts of the plant, while vincamine, vinceine, ajmalicine, catharanthine, etc. are found in the leaves and roots. These alkaloids have been widely used in applications such as pharmaceuticals, pesticides, agrochemicals, and food additives. In addition to alkaloids, different phenolic compounds are present in *C. roseus*, including C6C1 compounds, i.e., at least one carboxylic acid is attached to the aromatic ring. These compounds include

flavonoids, phenylpropanoids, such as derivatives of cinnamic acid, anthocyanins, and 2,3-dihydoxybenzoic acid [18]. So far, studies have found profound antioxidant [19], antifungal, anticancer [20], and antimicrobial [21] activities. Due to the presence of alkaloids such as resperin, ajamalicine, and serpentine, the plant is also known to possess antihypertensive and antispasmodic properties. As a result, this plant is an excellent candidate for use as a source of powerful antioxidants in the green synthesis of NPs.

To the best of our knowledge, so far there have been no reports of the synthesis of Cu/Ag/Zn nanoparticles from *C. roseus*. Therefore, in this work, the aqueous leaf extract of *C. roseus* was employed to synthesise a blend of copper (Cu), silver (Ag), and zinc (Zn) nanoparticles. Silver nanoparticles (Ag) have become more popular among noble metals as a result of their unique physiological properties, such as catalytic, magnetic, optical, electronic, and antibacterial functions, in comparison to bulk metal. Additionally, silver nanoparticles have been used in the creation of numerous topical antimicrobial creams, lotions, and gels that are both bactericidal and fungicidal, in biomedical materials such as catheters and wound dressings, and in biotechnological products such as water filters and activated carbon air filters. The enormous natural availability and inexpensive price of copper make Cu NPs particularly alluring. Cu-based nanocatalysts have several uses in nanotechnology due to their special traits and attributes, such as catalysing organic transformations, electrocatalysis, and photocatalysis. Cu NPs have been shown to have amazing antioxidant and antimicrobial properties in many of the studies performed. Cu and its alloys have historically been among the most valuable metals due to their special qualities, and this trend will continue in the future. Iron nanoparticles can easily aggregate small floccules of either millimetre or micron size due to their large specific high surface energy, magnetic interaction, and surface area. According to reports, zinc nanoparticles function as catalysts and reductants to remove pollutants such as arsenic, lead, chromium, and chlorinated solvents. Because of the unique properties of Zn NPs, they exhibit potential antioxidant activity as well. Therefore, these three metals were chosen as part of our study. The research work also involved evaluating the properties of the resulting nanoparticles, including their antioxidant activity and their effectiveness in catalysing the degradation of harmful dyes such as phenol red and eosin yellow.

An antioxidant is a chemical that inhibits cellular molecules from oxidising. Antioxidants are compounds, either natural or synthetic, that can prevent or delay oxidant-induced cell damage, including unstable molecules such as free radicals and reactive oxygen species (ROS) [22]. Oxidation is a common chemical process that enables hydrogen or electrons to be removed from a substance. During the biological oxidation reaction, free radicals are formed. As a result of the the reactive nature of the free radicals formed, they start a chain reaction at the same time, which can cause cellular damage or even death. The antioxidant potential of a heterocyclic or aromatic ring is determined by the number and location of the hydroxyl groups. For a substance to be classified as an antioxidant, it must satisfy several criteria. These include being effective at low concentrations, generating a less toxic final product after the reaction, having sufficient capacity to deactivate the targeted molecule, and being able to react with oxygen or nitrogen free radicals [23]. Because plants have medicinal characteristics that can be added to nanoparticles during synthesis, using them to create nanoparticles is useful. Plant phytocompounds have antioxidant properties that give nanoparticles even more antioxidant protection. The phenolic compounds present in *C. roseus* possess antioxidant properties. In this study, antioxidant activity was examined in trimetallic nanoparticles synthesised using leaf extracts obtained from *C. roseus.* Metal nanoparticles, including gold, copper, silver, and iron oxide, have been studied for their antioxidant potential. The antioxidant activity of these nanoparticles is attributed to their high surface area, which allows for greater interactions with free radicals and ROS, and their ability to donate or accept electrons, which can neutralise reactive species. Research has been conducted on nanoparticles made up of three different metals to determine their ability to act as antioxidants, and certain studies have demonstrated encouraging findings. Trimetallic nanoparticles typically consist of three different metallic elements, such as gold,

silver, and copper, and their antioxidant activity is thought to be due to the synergistic effects of these elements.

As a result of rapid industrialisation and urbanisation, renewable sources such as water resources are being polluted. Although more than 75% of our planet is covered by water, only about 5% of water resources are available for utilisation by living beings [24]. The leather, textile, cosmetics, and paper industries use dyes to impart colour to their products, which take time to degrade and are released into the water without being treated, resulting in environmental pollution [25]. As these dyes can be extremely carcinogenic, the distribution of untreated wastewater into waterways directly poses a significant risk to living beings, mainly aquatic organisms. Furthermore, due to their lack of biodegradability, these synthetic organic compounds must be processed prior to use [26]. Azo dyes are the most commonly used and the most hazardous dyes used in the textile and dyeing industries. At least one nitrogen atom is attached to the aromatic group, and the nitrogen is double-bonded (N=N). Various physical methods have been used for a long time to degrade these toxic dyes, such as reverse osmosis, absorption, and activated carbon. The aforementioned methods only lead to the movement of pollutants from one substance to another, causing contamination in the secondary medium. As a result, further treatment of solid waste and regeneration of the adsorbent is often required, thereby increasing the overall cost of the process [27]. Similarly, different chemical methods, for instance, chlorination and ozonation, are also used for the removal of dyes, but there are significant adverse effects due to the production of toxic metabolites that deteriorate the health of aquatic animals living in the water resources. Therefore, biological methods could be the most effective in eradicating toxic dyes from wastewater. This research focused on examining the catalytic breakdown of three dyes—methyl red, phenol red, and eosin yellow—using $NaBH_4$ with the assistance of nanoparticles. The nanoparticles were found to have improved physical and chemical characteristics, resulting in greater reactivity compared to larger materials.

2. Results and Discussions

UV–Vis studies of synthesised nanoparticles:

An efficient technique for keeping track of the development of a reaction or studying the surface plasmon resonance (SPR) of metal nanoparticles is ultraviolet–visible (UV–Vis) spectrophotometry [28]. It is a method by which light absorption passes through an experimental sample. Color change show the synthesis of nanoparticles (Figure 1). Both the ultraviolet and visible spectrums of light are energetic and capable of raising the energy level of electrons. In this study, the wavelength range of 200–800 nm was used to measure the absorbance (Figure 2). This analysis was carried out 24 h after the reaction.

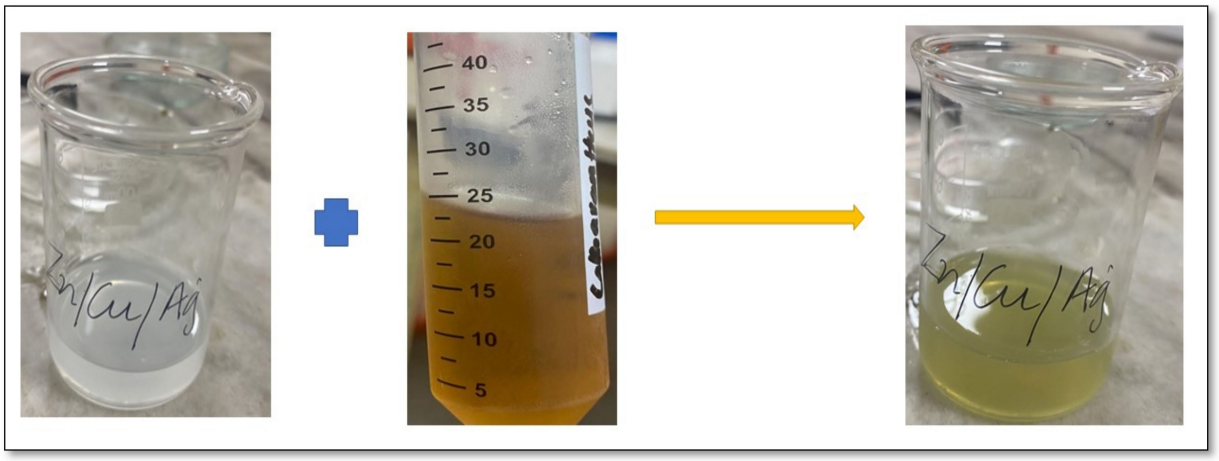

Figure 1. The colour of the metal precursor changed to greenish after the addition of leaf extract.

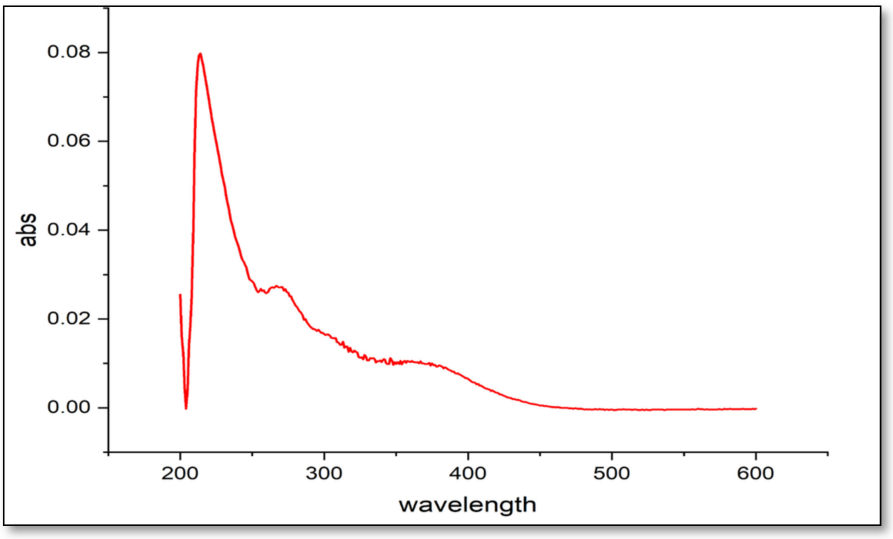

(**a**)

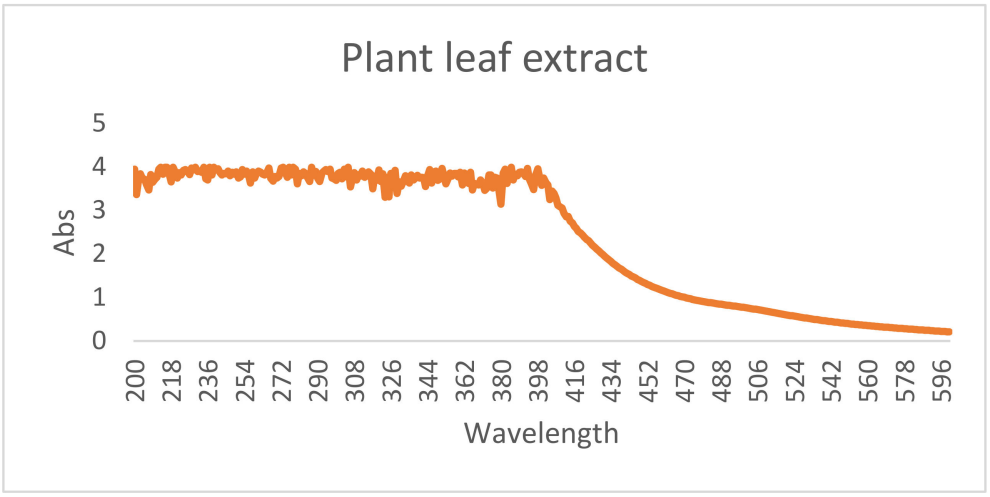

(**b**)

Figure 2. UV spectroscopy of (**a**) Cu/Ag/Zn nanoparticles and (**b**) plant leaf extract.

Three distinct peaks were observed during the UV–Vis analysis. An increase in the absorbance band was observed at a wavelength of 220 nm, which confirmed the presence of copper oxide (CuO). CuO NPs synthesised using *Enicostemma axillare* leaf extract showed a distinct peak at 234 nm [29]. In one study, CuO NPs were synthesised using *Carica papaya*, which was readily visible in the UV–Vis spectrum around 250 nm due to plasmon resonance [30]. Many other studies depicting the formation of CuO NPs observed a peak in a similar range. Another distinct peak at 270 nm was characteristic of zinc oxide (ZnO). The presence of a metal oxide (ZnO) was indicated by absorbance peaks at 230 and 270 nm in copper-doped ZnO nanoparticles in other research [31]. Furthermore, the presence of zinc ions was observed in the crystal lattices in an experiment, which led to a modification of the lattices, particularly in their extension. This modification caused an increase in the intensity of the absorbance peak after doping ZnO with Cu [32]. The absorbance band at 370 nm depicted the formation of Ag nanoparticles. A wide peak in the 400 nm region was recorded as a result of the silver nanoparticles synthesised using an aqueous extract of *Berberis vulgaris* leaf and root [33]. Furthermore, an intense SPR peak was observed at 390 nm in the biosynthesis of silver nanoparticles using sorghum bran extract [34]. These

findings were consistent with the results observed in the current study. During the synthesis of bimetallic Ag–ZnO NPs, a widened peak was discerned in the UV spectrum within the range of 400–450 nm [35]. This peak was attributed to the surface plasmon of silver and provided compelling evidence for the interaction between silver and zinc oxide.

FTIR studies of synthesised nanoparticles:

FTIR analysis was performed on both *C. roseus* leaf extract and the trimetallic nanoparticles synthesised from the extract (Figure 3). The analysis revealed a wider band within the range of 3000 to 3500 cm^{-1}, with a peak at 3331 cm^{-1}, indicating the presence of alcohols and phenols as well as the vibration of OH stretching. During the synthesis of palladium nanoparticles using *C. roseus* leaf extract, a similar result was observed where the FTIR spectrum showed an absorbance band in the 3453 cm^{-1} region, indicating the presence of OH groups [36]. Furthermore, silver nanoparticles synthesised using *Azadirachta indica* exhibited absorption peaks at around 3489.2 and 3293.1 cm^{-1}, which were assigned to the stretching vibrations of O–H. In addition, absorbance bands at 571.6, 534.8, and 661.5 cm^{-1} were reported, which were attributed to the presence of C–Cl and C–Br, indicating strong alkyl halides [37]. In another study, a stretch peak at 649 cm^{-1} was observed in the synthesis of Ag and TiO_2 nanoparticles using an aqueous leaf extract of *Euphorbia prostrata* [38]. Therefore, it is logical that the sharp peak observed at 665 cm^{-1} in this study was due to a halogen compound. One study in the literature suggested the representation of the carbonyl group (C=O) in the absorbance band at 1643 cm^{-1}, which was close to the absorbance peak at 1625 cm^{-1} in the current study, thus depicting the presence of the carbonyl group [39]. These results suggested the presence of phenols and flavonoids in the leaf extract, which likely played a role in the reduction of the metal precursors to their corresponding metal ions. Without other strong ligating agents present, polyphenolics can adsorb onto the surfaces of metal nanoparticles, possibly through pi-electron interactions. In a redox system, the pi-electrons of the carbonyl group (C=O) from the C ring of a flavonoid can transfer to the free orbital of a metal ion, converting it to its free metal form.

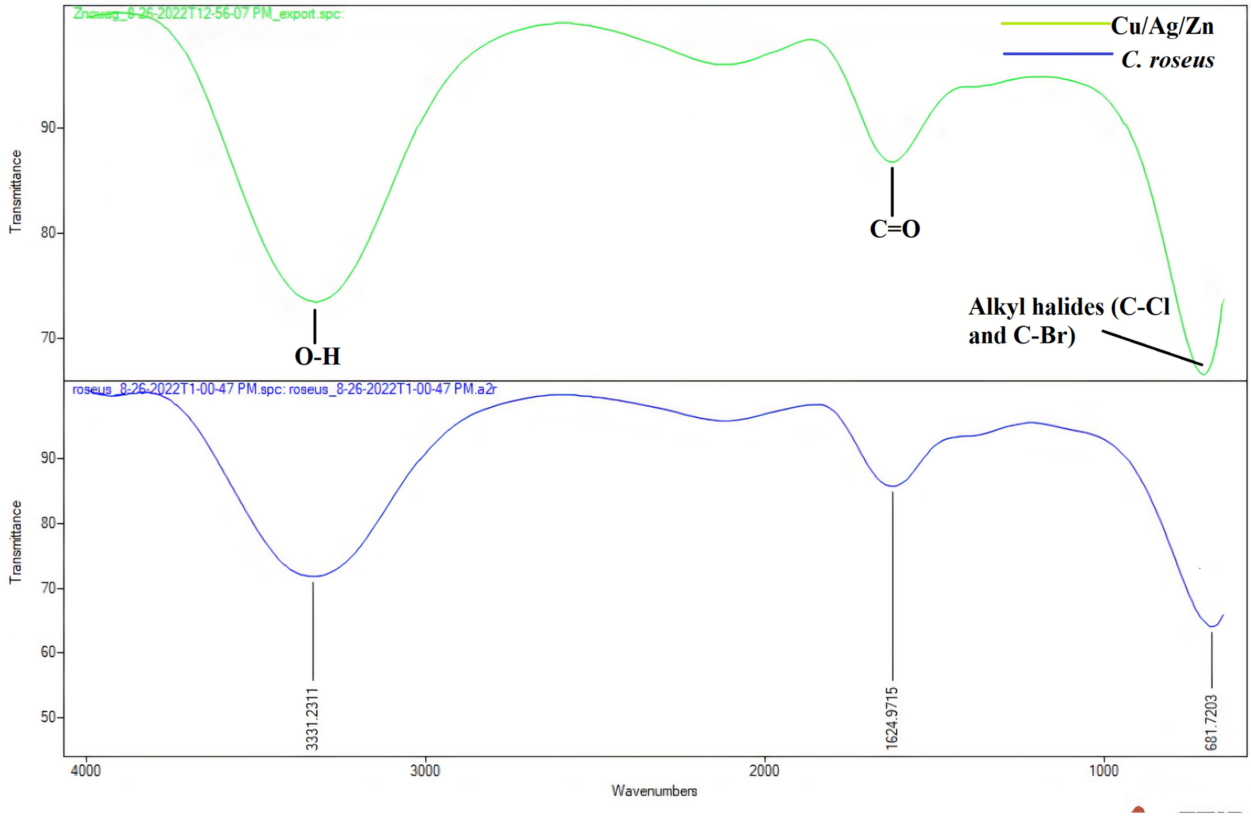

Figure 3. FTIR spectra of *C. roseus* extract and trimetallic Cu/Ag/Zn nanoparticles.

FTIR analysis was conducted to identify the functional groups present in the leaf extract that were responsible for the synthesis and stabilisation of the trimetallic nanoparticles through the bioreduction of metal ions. Figure 3 shows the FTIR spectrum of the trimetallic nanoparticles obtained from *C. roseus*, where strong peaks were observed at 3357, 1644, 728, and 691 cm^{-1}. A research study suggested that the strong peak at 1644 cm^{-1} indicated a C=O bond due to stretching vibrations in the carboxyl group or maybe the bending of C–N in the amide group [40]. In addition, the absorption band observed at 3357 cm^{-1} suggested the presence of stretching vibrations of the N–H/C–H/O–H bonds of amines, amides, and alcohols. The stretch of bands between 3000 and 3500 cm^{-1}, in which 3357 cm^{-1} demonstrated a sharp peak, could mean that the functional groups of flavonoids, caffeic acid, and cinnamic acid and its derivatives in the leaf extract of *C. roseus* were involved in the creation of the nanoparticles [41,42]. Furthermore, the absorbance band at 728 cm^{-1} depicted the presence of aromatic monosubstituted groups. The FTIR analysis of the trimetallic Zn/Cu/Ag NPs synthesised from the leaf extract revealed the presence of various functional groups related to active phytochemicals such as phenolic acids, flavonoids, aromatic compounds, etc. These groups are believed to be responsible for the reduction of metal precursors and the subsequent stabilisation of the produced trimetallic NPs. These phytochemicals present in the extract, mainly flavonoids and phenolic acids, could reduce the metal ions by donating electrons, leading to the formation of metal nanoparticles. Moreover, they could prevent the aggregation of nanoparticles by binding to the surface of the nanoparticles, creating a protective layer that reduced the surface energy and stabilised them. In addition, the carboxyl and hydroxyl groups could also bind to the metal ions on the surface of the nanoparticles and prevent further oxidation, helping to maintain their structural integrity.

DLS analysis:

The Cu/Ag/Zn nanoparticles had a hydrodynamic diameter of approximately 142 nm. In a study, silver NPs were synthesised using *Lippia nodiflora* extract and an average particle size of 143.7 nm was determined [43]. The researchers suggested that the presence of small amounts of larger particles, which resulted from agglomeration or contamination, may have contributed to the larger size and caused ambiguity in the particle size measurements. Similarly, in another study, while working on the biosynthesis of gold NPs using an extract of *Cofea arabica*, a particle size of approximately 500 nm was evaluated. They concluded that the value of the particle size was a result of the cloud of molecules created by the plant extract, as their interaction with the surface of the nanoparticle increased its hydrodynamic diameter [44]. The surface charge of the synthesised Cu/Ag/Zn nanoparticles was measured by zeta potential. Zeta potential values greater than +30 mV or less than −30 mV are typically thought to produce stable suspensions [45]. However, the surface charge of the NPS was found to be −8.94 mV. This may have been due to the agglomeration of synthesised NPs. Particles begin to aggregate when attraction outweighs repulsion, which progressively affects the zeta potential value. The development of negative zeta potential values was due to the binding of functional groups to the surface of NPs. Similarly, a zeta potential of 4.8 mV was recorded when zinc oxide NPs were created using the stem bark extract of *Boswellia ovalifoliolata* in one study. The authors came to the conclusion that this meant that the zinc nanoparticles were subject to repellent electrostatic forces [46]. Figure 4a,b shows the particle size and zeta potential of the synthesised nanoparticles, respectively.

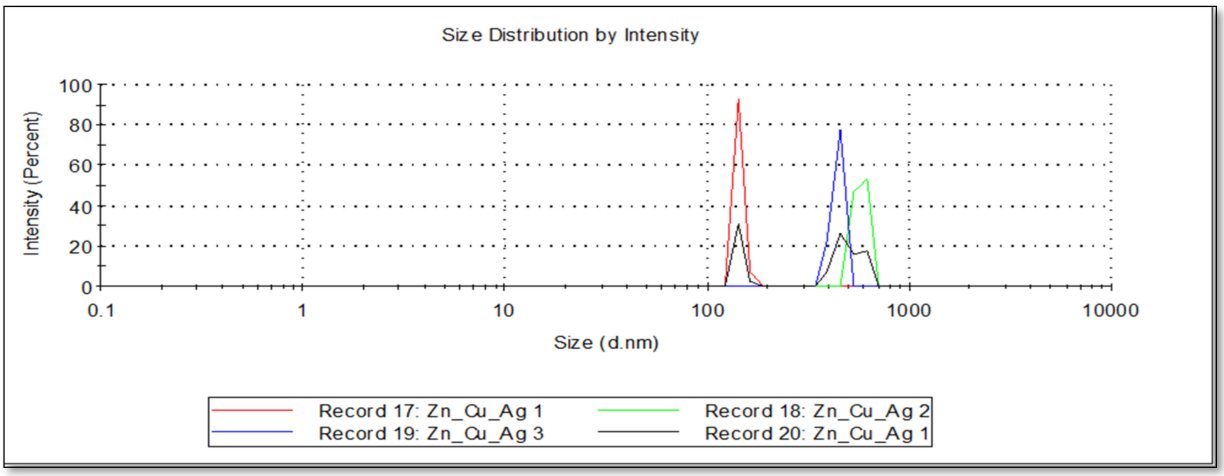

(**a**)

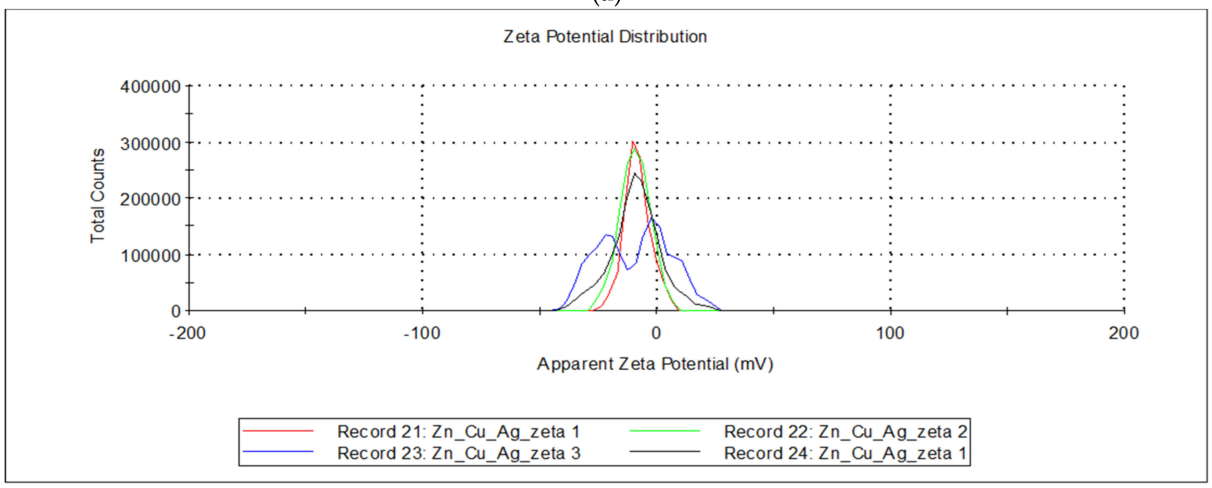

(**b**)

Figure 4. (**a**) Particle size of Cu/Ag/Zn nanoparticles. (**b**) Zeta potential of Cu/Ag/Zn nanoparticles.

XRD analysis:

The exact crystalline nature of the biogenic trimetallic nanoparticles was deduced by XRD analysis. X-ray diffraction (XRD) analysis is a technique used to identify the crystal structure and phase composition of materials, including metal nanoparticles. In this technique, a beam of X-rays is directed onto the surface of the material and the resulting diffraction pattern is analysed to determine the crystal structure and phase composition of the material. The average particle size was calculated from the width of the diffraction peaks using the Debye-Scherrer formula:

$$D = 0.94\lambda/\beta\cos\theta$$

where λ is the wavelength of the X-rays used, equal to 0.15418 Å; β is the full width at half maximum height measured in radians, which determines the spectral resolution; and θ is Bragg's diffraction angle measured in degrees. The average crystallite size was found to be 34.67 nm. A high level of crystallinity was observed in the sample, which had diffraction angles of 26.1995 and 27.8029 that could be indexed at (210) and (111), respectively, corresponding to the characteristic face-centred cubic of copper (Figure 5) (Table 1). The signals at 31.6839, 32.2832, and 32.8055 could be indexed at (100) and (002), which corresponded to the characteristic hexagonal-shaped zinc crystal. The data obtained were compared to card no. 01-080-3002 in the ICDD PDF standard database [43].

The diffraction angles observed at 38.1354 and 46.2701 were indexed to (111) and (200), respectively, which corresponded to the crystalline facets of silver [44].

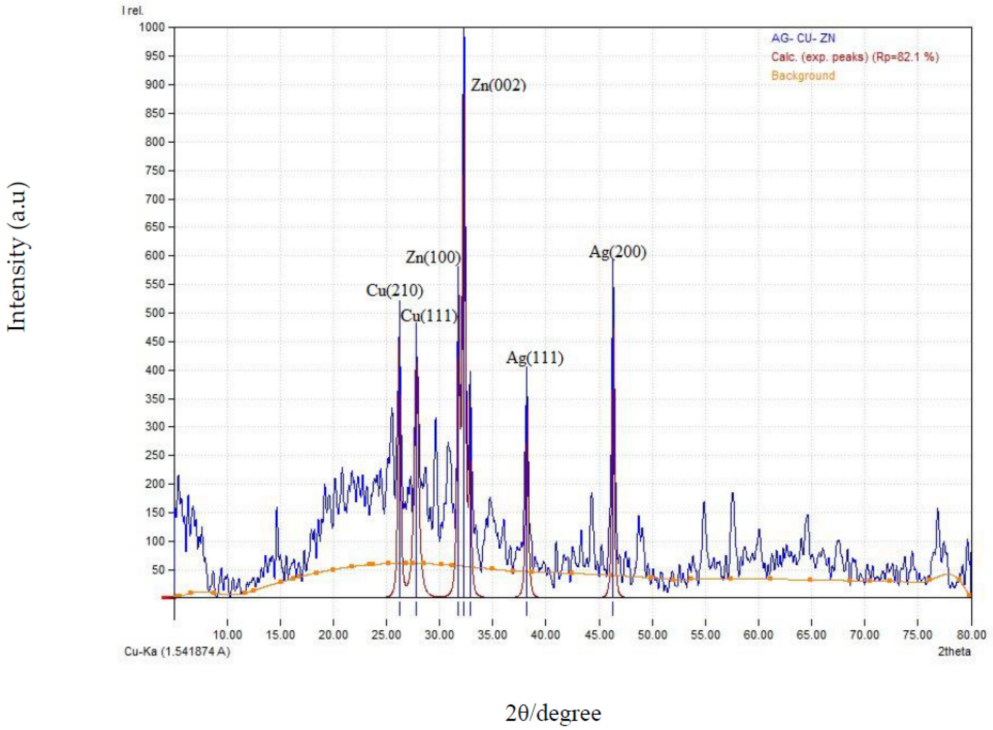

Figure 5. Graph representing the XRD pattern of intensity (*y*-axis) versus diffraction angle (2θ) (*x*-axis).

Table 1. XRD Analysis.

S. N	2θ (°)	Height (CTS)	FWHM (Radians)	Crystalline Size (nm)
1	26.1995	52.68	0.0051190507	27.88
2	27.8029	81.9	0.0051190507	28
3	31.6839	51.31	0.00204901654	70.48
4	32.2832	102.32	0.00654149404	22.11
5	32.8055	41.64	0.005119	28.27
6	38.1354	57.45	0.005119	28.697
7	46.2701	77.08	0.004044	37.32

SEM-EDX:

The presence of Cu, Ag, and Zn was confirmed by SEM-EDX analysis, which is shown in the figure given below. The SEM micrographs of the trimetallic Cu/Ag/Zn nanoparticles biosynthesised using the leaf extract of *C. roseus* showed irregular shapes (Figures 6 and 7). One reason for the observation of irregular shapes could be the tendency of biologically synthesised metal nanoparticles to aggregate. The composition of each element is shown in the table below. The EDX spectrum of the synthesised trimetallic nanoparticles showed strong copper, silver, and zinc signals. The presence of surface-bound biomolecules or phytochemicals that served as surface capping or stabilising agents may have been indicated by the presence of modest C and O signals among the other signals present in the EDX analysis. The synthesised trimetallic NPs had a compositional atomic ratio of 1:1.46:1.05 (Cu:Ag:Zn), which deviated from the standard stoichiometric ratio used to synthesise them. This may have been caused by variations in the NP surface energies or by the particular crystallographic orientation of the metal atoms.

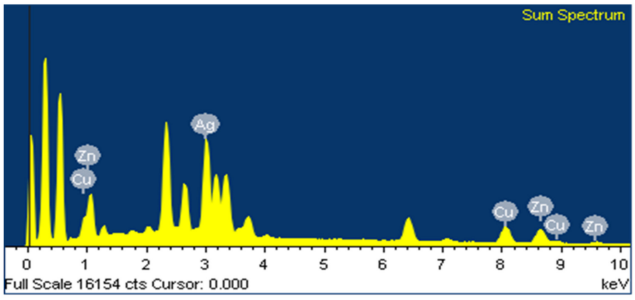

Element	Weight%	Atomic%
Cu K	21.84	28.37
Zn K	23.79	30.03
Ag L	54.37	41.60
Totals	100.00	

Figure 6. EDX spectrum of synthesised nanoparticles.

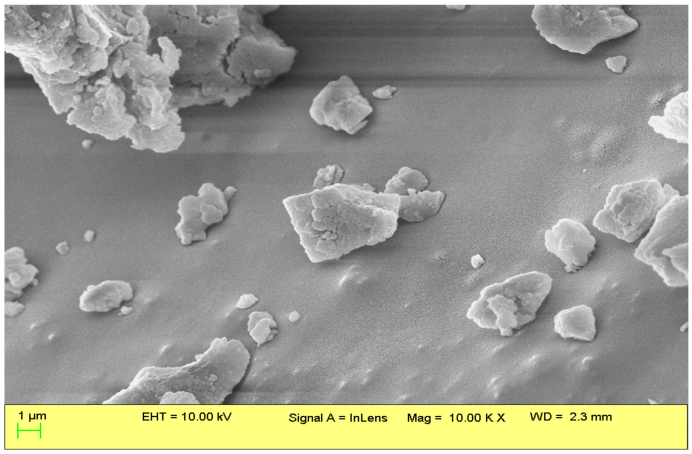

Figure 7. SEM image at 10X magnification.

Antioxidant activity:

The physical and chemical properties of trimetallic nanoparticles make them unique, and their potential antioxidant activities were studied using the DPPH assay. The DPPH (2,2-diphenyl-1-picrylhydrazyl) assay is a widely used method to determine the antioxidant activity of different compounds, including metal nanoparticles (Figure 8). In this assay, DPPH, a stable free radical, is reduced to a nonradical form in the presence of an antioxidant, resulting in a change in colour from purple to yellow in a concentration-dependent manner. The unique physical and chemical properties of trimetallic nanoparticles, such as their high surface area-to-volume ratio and small size, make them highly efficient in electron transfer and allow them to easily penetrate cells and tissues. In addition, these nanoparticles have the ability to scavenge reactive oxygen species (ROS), which are highly reactive molecules that can cause damage to cells and contribute to oxidative stress.

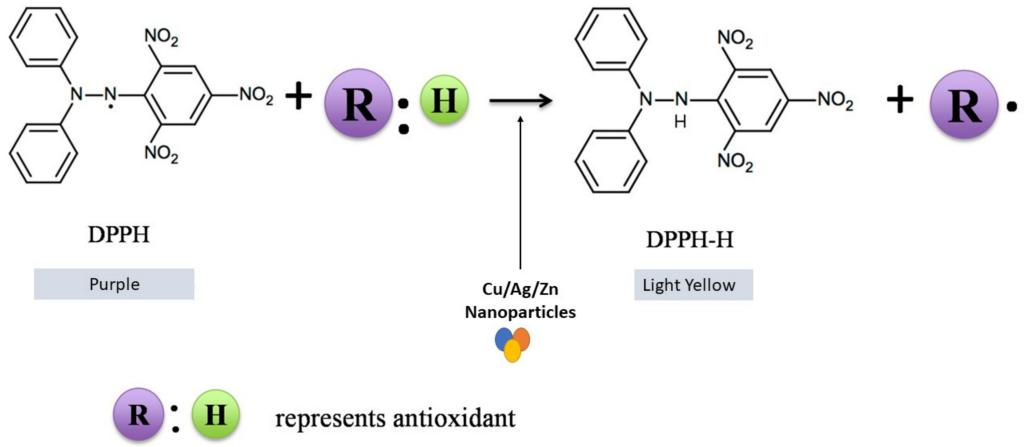

Figure 8. Antioxidant activity of Cu/Ag/Zn nanoparticles.

To determine the antioxidant activity of the Cu/Ag/Zn nanoparticles (NPs), a DPPH assay was performed in which ascorbic acid was used as a positive control (Figure 9). The activity was observed to be 36.07%, 35.73%, 37.06%, 35.96%, 35.51%, 37.29%, and 68.03% at 10, 50, 100, 150, 200, 500, and 1000 µg/mL, respectively (Figure 10). The results suggested that the antioxidant properties of the Cu/Ag/Zn nanoparticles were more significant than those of ascorbic acid, a known antioxidant, at lower concentrations (10 µg/mL). Furthermore, at higher concentrations (1000 µg/mL), the Cu/Ag/Zn nanoparticles exhibited remarkably high antioxidant activity compared to lower concentrations.

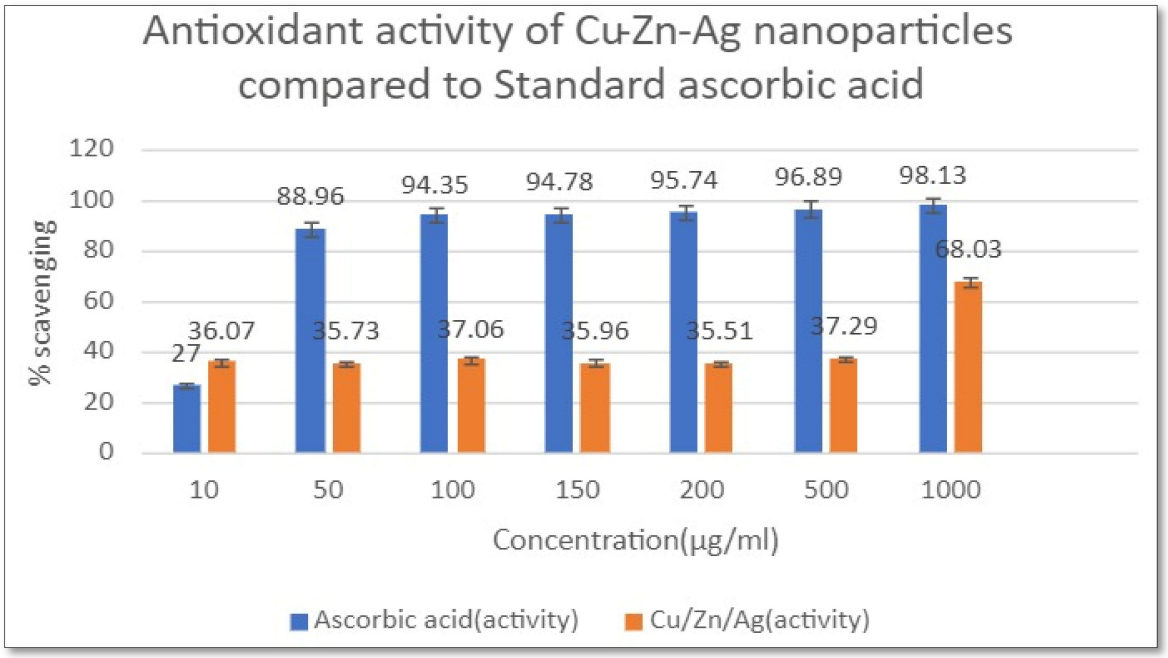

Figure 9. Antioxidant activity of standard ascorbic acid vs. Cu/Ag/Zn NPs.

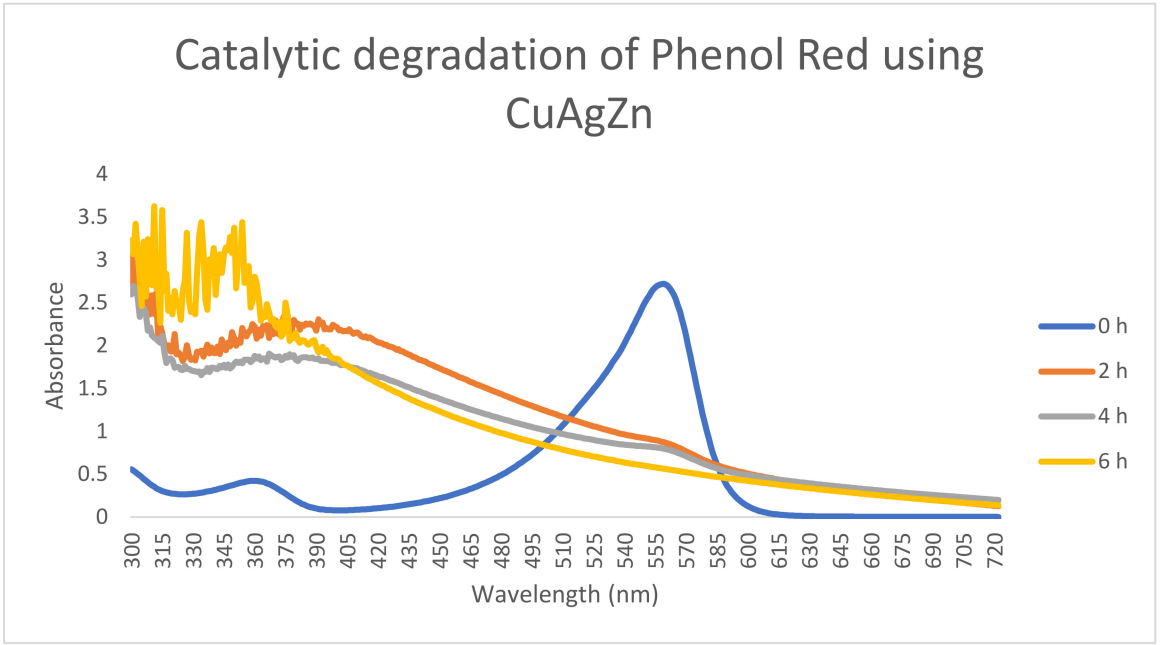

Figure 10. UV–Vis absorption spectra of phenol red in the presence of biogenic Cu/Ag/Zn nanoparticles together with $NaBH_4$ at different time intervals.

The synthesis, characterisation, and antioxidant and antibacterial activity of copper nanoparticles were reported in a study using *C. vitiginea* leaf extract. The antioxidant activity of the synthesised copper nanoparticles was recorded to be 21% [47]. The antioxidant activity shown by the nanoparticles could be traced back to the various types of alkaloids present in *C. roseus*, the extract of which was used in the biosynthesis of the NPs. In addition to the terpenoid indole alkaloid, *C. roseus* synthesises over 150 terpenoid indole alkaloids and a diverse range of phenolic compounds, such as caffeic acid flavonoids, and cinnamic acid and its derivatives [48]. The antioxidant activity of phenolic compounds has been attributed to several mechanisms, and different methods are available to assess the antioxidant properties of lignins and tannins present in phenolic acids. The presence of one or two methoxy groups in the ring increases the antioxidant activity of compounds with one hydroxyl group. When an electron donor group, such as an alkyl or methoxy group, is introduced into the ortho position, the antioxidant properties of phenolic acids are strengthened [49]. The synthesis, characterisation, and antioxidant and antibacterial activity of copper nanoparticles were reported in a study using *C. vitiginea* leaf extract. The antioxidant activity of the synthesised copper nanoparticles was recorded to be 21% [47]. Silver nanoparticles have been reported to exhibit antioxidant activity due to their ability to scavenge free radicals. For example, in one study, silver nanoparticles synthesised using garlic extract exhibited strong antioxidant activity, which was attributed to their large surface area and unique physicochemical properties [50]. Nevertheless, there is limited research on trimetallic nanoparticles as antioxidants, although a few studies have reported their potential as antioxidant agents. In another study, trimetallic gold/silver/copper nanoparticles were synthesised, and their antioxidant activity was evaluated using the DPPH assay. The nanoparticles exhibited strong antioxidant activity, with higher scavenging activity than individual gold, silver, and copper nanoparticles [51]. There are numerous studies available in the field of nanotechnology depicting the antioxidant activity of metal nanoparticles using various medicinal plants. However, there is no report of the synthesis of Cu/Ag/Zn nanoparticles using *C. roseus*. Hence, this study aimed to investigate the antioxidant activity of these Cu/Ag/Zn NPs.

Catalytic degradation of phenol red:

Phenol red is a pH indicator that is commonly used in cell culture and microbiology. It is a yellowish-red crystalline powder that turns from yellow to pink to red depending on the pH of the solution. The degradation of phenol red can be challenging, depending on the method and conditions used for its degradation. Phenol red is a persistent organic compound that is relatively stable and difficult to degrade by natural processes. For example, high concentrations of phenol red and other organic compounds may be present in industrial wastewater treatment, making their degradation more challenging. Therefore, some degree of effort and expertise is required to break down its chemical structure and reduce it to harmless by-products. The use of nanoparticles for the degradation of phenol red can be an effective approach. There have been studies on the use of trimetallic nanoparticles for the degradation of phenol red in aqueous solutions. One study found that biologically synthesised zinc oxide (ZnO) nanoparticles using a methanolic leaf extract of *C. roseus* were effective in degrading phenol red within 8 h after the addition of the ZnO nanoparticles [40].

Figure 10 shows the UV absorption spectra of phenol red after the addition of trimetallic Cu/Ag/Zn nanoparticles over time. When treated with only $NaBH_4$, the dye showed an insignificant reduction. Synthesised biogenic trimetallic nanoparticles exhibited very good phenol red degradation, almost up to 78%, in the presence of $NaBH_4$ (Figure 10). The maximum absorption intensity of phenol red was recorded at 560 nm. The larger peak shown in the graph may have reflected the formation of intermediates such as hydrazines following the addition of the nanoparticles and $NaBH_4$. The absorption intensity decreased with an increase in time. In fact, 6 h after the addition of biogenic NPs, the maximum reduction in absorption was observed. The mechanism of degradation of phenol red by trimetallic nanoparticles involved the generation of reactive oxygen species (ROS) such as

hydroxyl radicals, which broke down the phenol red molecule into smaller and less toxic compounds (Figure 11). The study results suggested that the trimetallic nanoparticles have potential for use in the degradation of phenol red and may offer a promising solution for the remediation of environments contaminated with this dye.

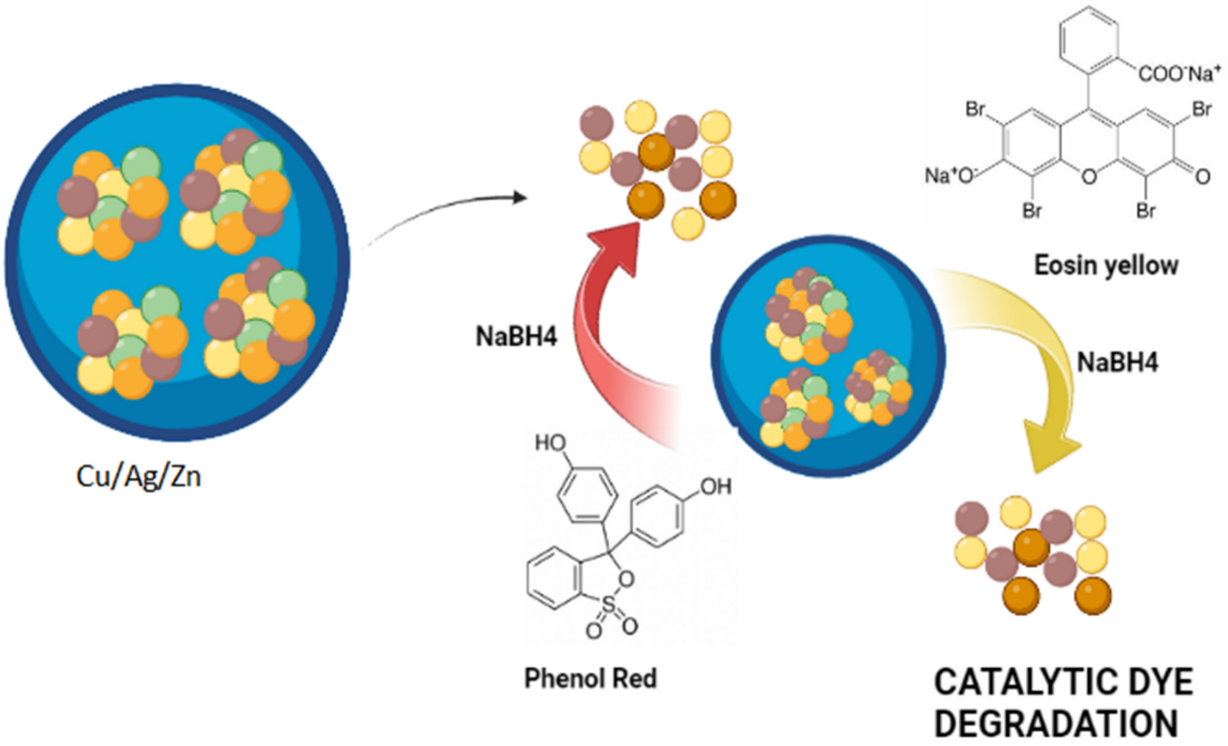

Figure 11. Dye degradation using Cu/Ag/Zn nanoparticles.

Catalytic degradation of eosin yellow:

Metal nanoparticles have been studied extensively for their potential to degrade pollutants and environmental contaminants, including dyes such as eosin yellow. Eosin yellow is an anionic dye that can cause severe damage to the gastrointestinal and respiratory tracts. It is also an irritant to the skin and eyes [52]. Eosin yellow is a synthetic organic dye commonly used in the textile, food, and cosmetic industries. It is a potential environmental contaminant due to its toxicity and persistence in water bodies. Metal nanoparticles such as iron, silver, gold, and copper have been found to effectively degrade eosin yellow through various mechanisms, including photocatalysis, electrocatalysis, and catalytic reduction. For example, iron nanoparticles synthesised using *Dimocarpus longan* have been shown to degrade eosin yellow through a process called the Fenton-like reaction, in which the nanoparticles catalyse the formation of highly reactive hydroxyl radicals that oxidise dye molecules [53].

In the present study, the absorption spectrum for eosin yellow showed a peak at 515 nm. The percentage of degradation of eosin yellow was found to be 50.7% after the addition of biogenic Cu/Ag/Zn nanoparticles (Figure 12). The results clearly showed that when eosin yellow was reduced in the presence of $NaBH_4$, the intensity of the absorbance peak decreased as the reduction progressed. The use of $NaBH_4$ (sodium borohydride) as a reducing agent has been explored in the degradation of eosin yellow using metal nanoparticles. $NaBH_4$ is a powerful reducing agent that can donate electrons to metal nanoparticles, leading to the reduction of pollutant molecules. This process can be used to break down eosin yellow into simpler, less toxic compounds. Several studies have reported the degradation of eosin yellow using metal nanoparticles and $NaBH_4$. For example, the catalytic degradation of eosin yellow using silver nanoparticles and $NaBH_4$ was demonstrated. The study showed that the degradation efficiency increased with the

addition of silver nanoparticles. The authors also suggested that the degradation improved with a decrease in the particle size of the silver nanoparticles [25].

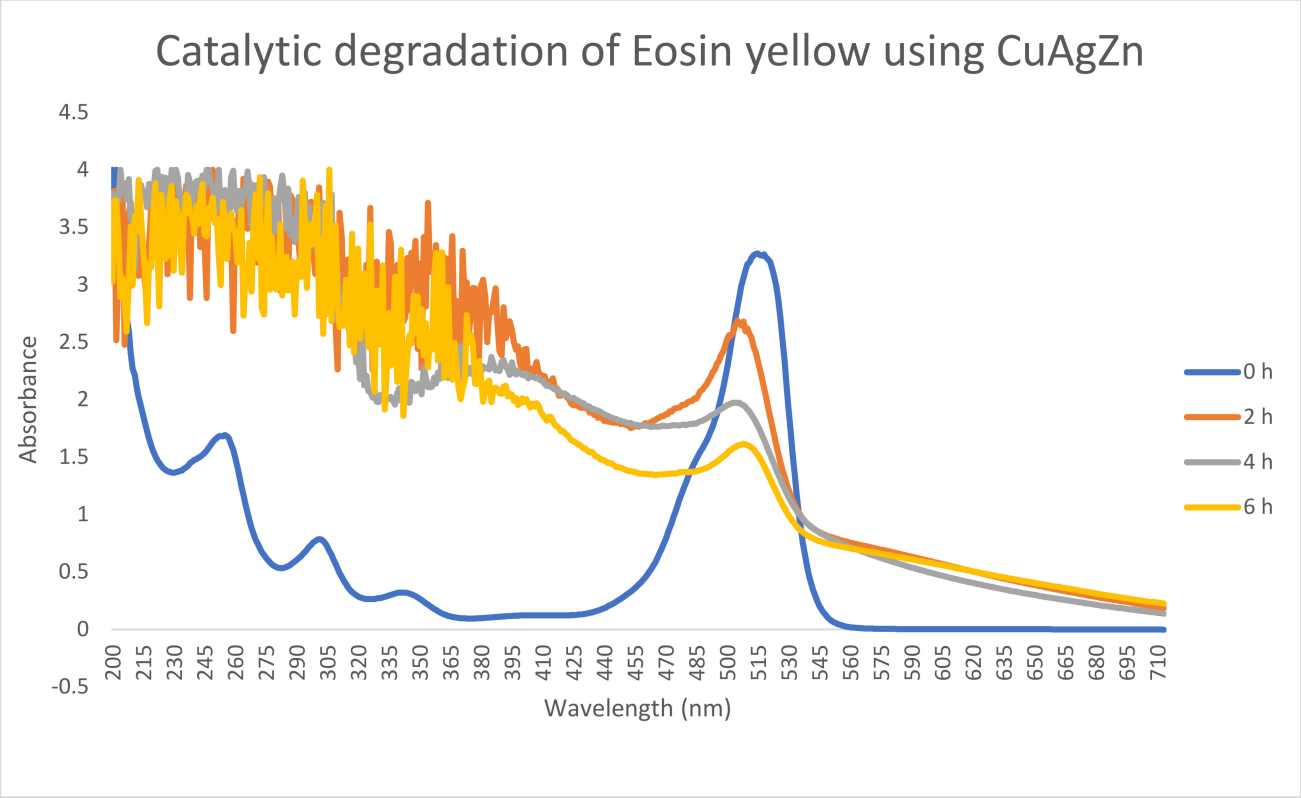

Figure 12. UV–Vis absorption spectra of yellow eosin in the presence of biogenic Cu/Ag/Zn nanoparticles along with $NaBH_4$ at different time intervals.

Trimetallic nanoparticles can be a promising approach for the degradation of eosin yellow in aqueous solutions. The use of trimetallic nanoparticles is based on the synergistic effect of combining different metals, which can lead to enhanced catalytic activity and efficiency for pollutant degradation. An example of trimetallic nanoparticles used for eosin yellow degradation is a combination of Fe/Pd/Cu nanoparticles. In a study, the degradation of eosin yellow was investigated using Fe/Pd/Cu nanoparticles and hydrogen peroxide (H_2O_2). The results showed that the trimetallic nanoparticles had superior catalytic degradation activity compared to that of binary or single-metal nanoparticles. The degradation efficiency reached 99.5% after 120 min of reaction time, which was attributed to the synergistic effect of the three metals in the nanoparticles [54]. Similarly, in another study, the degradation of eosin yellow was achieved using trimetallic Fe/Ni/Pd nanoparticles. The study showed that the degradation efficiency increased with increasing nanoparticle dosage and decreasing pH. The authors suggested that the degradation mechanism involved the generation of hydroxyl radicals through the Fenton-like reaction between Fe and H_2O_2, and the surface reaction between eosin yellow and metal nanoparticles [55].

These studies demonstrate the potential of trimetallic nanoparticles for the degradation of eosin yellow and other pollutants in aqueous solutions. The combination of multiple metals in the nanoparticles can lead to enhanced catalytic activity and synergistic effects, which can improve the efficiency of the degradation process.

3. Material and Methods

Distilled water was utilised as a solvent for the production of plant extracts and salt solutions. Metal precursor salts, namely silver nitrate ($AgNO_3$) with a molecular weight of 169.87 g/mol, copper (II) sulphate pentahydrate ($CuSO_4 \cdot 5H_2O$) with a molecular

weight of 249.68 g/mol, and zinc sulphate heptahydrate ($ZnSO_4 \cdot 7H_2O$) with a molecular weight of 287.6 g/mol, were acquired from the Department of Biotechnology Laboratory of Sharda University, Greater Noida, India. The leaves of *C. roseus* were obtained from nearby plants. Furthermore, 1,1-diphenyl-2-picrylhydrazyl (DPPH) with a molecular weight of 394.32 g/mol and L-ascorbic acid ($C_6H_8O_6$) with a molecular weight of 176.12 g/mol were also obtained from the laboratory. The DPPH solution was prepared using ethanol as the solvent, which was obtained from the laboratory.

3.1. Preparation of Extract

Labolin was used to clean the *C. roseus* leaves, which were then rinsed with distilled water to remove any impurities and dust particles from the surface. Subsequently, the leaves were dried in a hot air oven and ground into a fine powder with a mortar and pestle. Subsequently, 5 g of fine powder was added to a 250 mL beaker and dissolved in 100 mL of distilled water. The solution was then subjected to a 50 °C water bath for an hour. After cooling, the mixture was filtered using Whatman Filter Paper No. 1, and the extract was stored in a falcon tube for use in nanoparticle synthesis.

3.2. Preparation of Salt Solutions

The 10 mM stock solutions of all three metal salts were prepared by dissolving them in distilled water. First, 0.2876 g of $ZnSO_4 \cdot 7H_2O$ (molecular weight = 287.6 g/mol) was dissolved in distilled water to make 100 mL of 10 mM zinc sulphate salt solution. Similarly, 0.2496 g of $CuSO_4 \cdot 5H_2O$ (molecular weight = 249.68 g/mol) was dissolved in distilled water to make 100 mL of 10 mM copper sulphate salt solution. Then, 0.1698 g of $AgNO_3$ (molecular weight = 169.87 g/mol) was also dissolved in distilled water to make 100 mL of silver nitrate solution. The stock solutions were stored in a refrigerator for further use.

3.3. Preparation of Cu/Ag/Zn Nanoparticles

The trimetallic nanoparticles with Cu/Ag/Zn were synthesised in a typical reaction procedure by placing equal volumes of the metal precursor solutions of Cu (10 mM, 20 mL), Ag (10 mM, 20 mL), and Zn (10 mM, 20 mL) in a 250 mL beaker. A 20 mL aliquot of aqueous *C. roseus* leaf extract was added to this metal precursor reaction mixture until a dark greenish colour was observed indicating the formation of trimetallic nanoparticles, making the solution ratio 1:1:1:1. The solution was then kept overnight in a shaker incubator at 50 °C to achieve a homogenous mixture.

3.4. Preparation of Powderered Nanoparticles

The powdered nanoparticles were prepared simply by simply heating the aqueous solution of the nanoparticles at 70 °C for 1 h in a glass Petri dish. The resultant solid form of these nanoparticles was scraped from the glass Petri dish and collected in an Eppendorf tube.

3.5. Catalysis

Using $NaBH_4$, the biologically synthesised trimetallic Cu/Ag/Zn nanoparticles were used to degrade the harmful dyes eosin yellow and phenol red. A test tube was filled with 1.4 mL of water, 0.3 mL of 0.5 mM aqueous dye, and 1 mL of freshly prepared 0.03 M $NaBH_4$ solution. Then, 1 mL of biogenic Cu/Ag/Zn NPs was added, and spectroscopic assessment of the degradation reaction was conducted at regular intervals. Moreover, control tests without the trimetallic nanocatalysts were also performed. The degradation efficacy was determined by the equation:

$$\% \text{ degradation} = \{(A_0 - At)/A_0\} \times 100$$

where A_0 = absorbance at 0 min; At = absorbance at t minutes.

3.6. Characterisation of Synthesised Nanoparticles

The optical properties of the synthesised trimetallic nanoparticles were determined by measuring their UV–Vis (ultraviolet–visible light) absorbance spectra over a range of 200–800 nm. For this characterisation, the synthesised nanoparticle solution was diluted 100 times to give a clear reading. Fourier-transform infrared (FTIR) spectroscopy was used to examine the physicochemical properties of the synthesised trimetallic nanoparticles, which were synthesised using the leaf extract of *C. roseus*, and to determine their binding properties. Additionally, dynamic light scattering (DLS) was employed to ascertain the particle size and zeta potential of the synthesised trimetallic nanoparticles.

3.7. Evaluation of the Antioxidant Activity of Synthesised Nanoparticles

To determine the antioxidant potency of the synthesised trimetallic nanoparticles, the 1,1-diphenyl-2-picrylhydrazyl radical (DPPH) assay was used with L-ascorbic acid as the standard. A 0.3 mM DPPH-reagent solution was prepared by dissolving 11.8 mg of DPPH in ethanol to make 100 mL. To prepare the standard ascorbic acid solution with a concentration of 1 mg/mL, 100 mg of ascorbic acid was dissolved in 100 mL of ethanol. It was then diluted to different concentrations (10, 50, 100, 150, and 200 µg/mL) to perform the assay. Similarly, different concentrations (10, 50, 100, 150, 200 µg/mL, and so on) of synthesised nanoparticles were also prepared in ethanol. A 3 mL volume of the standard or the nanoparticle solution was mixed with 1 mL of DPPH and incubated in a dark room for 30 min. The absorbance was recorded at 517 nm for the prepared solution. A 1 mL volume of DPPH diluted to 4 mL with ethanol was taken as a positive control. The antioxidant activity was determined by calculating the percentage (%) of inhibition using the following formula:

$$\text{Scavenging effect (\%)} = [(A_c - A_s)/A_c] \times 100$$

where A_c represents the absorbance of the control and A_s represents the absorbance of the sample.

4. Conclusions

A simple, safe, and environmentally friendly method was used for the synthesis of trimetallic Cu/Ag/Zn nanoparticles using a leaf extract of *C. roseus*. The synthesis of these trimetallic nanoparticles was characterised by UV–Vis, FTIR, and DLS analysis. The antioxidant activity of these trimetallic nanoparticles was studied. A comparative analysis of antioxidant activity was performed between ascorbic acid (standard control) and the biosynthesised trimetallic nanoparticles. The antioxidant assessment of the synthesised trimetallic nanoparticles showed excellent radical scavenging activity (75.76%) at 1000 µg/mL. Furthermore, the biogenic trimetallic nanoparticles showed effective catalytic degradation activity against red phenol and eosin yellow. The use of biosynthetic procedures opens up new avenues for the development of ideal catalysts with high activity and stability.

Author Contributions: Conceptualization, A.R.; methodology, S.K., A.R. and U.B.; formal analysis, A.G. and M.M.S.A.; investigation, A.R., S.K. and U.B.; resources, P.S., K.K.Y. and S.R.; writing—original draft preparation, A.R., S.K. and U.B.; writing—review and editing, N.C., V.K.D., H.-K.P. and B.-H.J.; funding acquisition, H.-K.P. and B.-H.J. All authors have read and agreed to the published version of the manuscript.

Funding: This research received no external funding.

Data Availability Statement: Not applicable.

Acknowledgments: The King Saud University authors acknowledge the financial support through Researchers Supporting Project number (RSPD2023R688), King Saud University, Riyadh, Saudi Arabia This work was also supported by the Mid-Career Researcher Program [grant no. 2020R1A2C3004237] through the National Research Foundation of the Republic of Korea.

Conflicts of Interest: The authors state no conflict of interest.

References

1. Sharma, G.; Kumar, D.; Kumar, A.; Ala'a, H.; Pathania, D.; Naushad, M.; Mola, G.T. Revolution from monometallic to trimetallic nanoparticle composites, various synthesis methods and their applications: A Review. *Mater. Sci. Eng.* **2017**, *71*, 1216–1230. [CrossRef] [PubMed]
2. Vafaee, M.; Ghamsari, M.S. Preparation and characterization of ZnO nanoparticles by a novel sol–gel route. *Mater. Lett.* **2007**, *61*, 3265–3268. [CrossRef]
3. Swihart, M.T. Vapor-phase synthesis of nanoparticles. *Curr. Opin. Colloid Interface Sci.* **2003**, *8*, 127–133. [CrossRef]
4. Lastra, G.; Luque, P.A.; Quevedo-Lopez, M.A.; Olivas, A. Electrical properties of p-type ZnTe thin films by immersion in Cu solution. *Mater. Lett.* **2014**, *126*, 271–273. [CrossRef]
5. Musschoot, J.; Xie, Q.; Deduytsche, D.; Van den Berghe, S.; Van Meirhaeghe, R.L.; Detavernier, C. Atomic layer deposition of titanium nitride from TDMAT precursor. *Microelectron. Eng.* **2009**, *86*, 72–77. [CrossRef]
6. Capek, I. Preparation of metal nanoparticles in water-in-oil (w/o) microemulsions. *Adv. Colloid Interface Sci.* **2004**, *110*, 49–74. [CrossRef]
7. Amendola, V.; Meneghetti, M. Laser ablation synthesis in solution and size manipulation of noble metal nanoparticles. *Phys. Chem. Chem. Phys.* **2009**, *11*, 3805–3821. [CrossRef]
8. Majerič, P.; Rudolf, R. Advances in ultrasonic spray pyrolysis processing of noble metal nanoparticles. *Materials* **2020**, *13*, 3485. [CrossRef]
9. Khani, R.; Roostaei, B.; Bagherzade, G.; Moudi, M. Green synthesis of copper nanoparticles by fruit extract of *Ziziphus spina-christi* (L.) Willd.: Application for adsorption of triphenylmethane dye and antibacterial assay. *J. Mol. Liq.* **2018**, *255*, 541–549. [CrossRef]
10. Vaseghi, Z.; Nematollahzadeh, A.; Tavakoli, O. Green methods for the synthesis of metal nanoparticles using biogenic reducing agents: A review. *Rev. Chem. Eng.* **2018**, *34*, 529–559. [CrossRef]
11. Sunny, N.E.; Mathew, S.S.; Chandel, N.; Saravanan, P.; Rajeshkannan, R.; Rajasimman, M.; Vasseghian, Y.; Rajamohan, N.; Kumar, S.V. Green synthesis of titanium dioxide nanoparticles using plant biomass and their applications—A review. *Chemosphere* **2022**, *300*, 134612. [CrossRef] [PubMed]
12. Abdel-Rahman, L.H.; Al-Farhan, B.S.; Abou El-ezz, D.; Abd–El Sayed, M.A.; Zikry, M.M.; Abu-Dief, A.M. Green biogenic synthesis of silver nanoparticles using aqueous extract of *Moringa oleifera*: Access to a powerful antimicrobial, anticancer, pesticidal and catalytic agents. *J. Inorg. Organomet. Polym. Mater.* **2022**, *32*, 1422–1435. [CrossRef]
13. Park, J.H.; Ahn, H.S. Electrochemical synthesis of multimetallic nanoparticles and their application in alkaline oxygen reduction catalysis. *Appl. Surf. Sci.* **2020**, *504*, 144517. [CrossRef]
14. Karthikeyan, B.; Loganathan, B. Strategic Green Synthesis and Characterization of Au/Pt/Ag Trimetallic Nanocomposites. *Mater. Lett.* **2012**, *85*, 53–56. [CrossRef]
15. Guo, X.; Li, X.; Lai, C.; Jiang, X.; Li, X.; Shu, Y. Facile approach to the green synthesis of novel ternary composites with excellent superhydrophobic and thermal stability property: An expanding horizon. *Chem. Eng. J.* **2017**, *309*, 240–248. [CrossRef]
16. Mahmoudi, B.; Soleimani, F.; Keshtkar, H.; Nasseri, M.A.; Kazemnejadi, M. Green synthesis of trimetallic oxide nanoparticles and their use as an efficient catalyst for the green synthesis of quinoline and spirooxindoles: Antibacterial, cytotoxicity and anti-colon cancer effects. *Inorg. Chem. Commun.* **2021**, *133*, 108923. [CrossRef]
17. Kamli, M.R.; Srivastava, V.; Hajrah, N.H.; Sabir, J.S.; Hakeem, K.R.; Ahmad, A.; Malik, M.A. Facile Bio-Fabrication of Ag-Cu-Co Trimetallic Nanoparticles and Its Fungicidal Activity against *Candida auris*. *J. Fungi.* **2021**, *7*, 62. [CrossRef]
18. Mustafa, N.R.; Verpoorte, R. Phenolic compounds in *Catharanthus roseus*. *Phytochem. Rev.* **2007**, *6*, 243–258. [CrossRef]
19. Jaleel, C.A.; Gopi, R.; Lakshmanan, G.A.; Panneerselvam, R. Triadimefon induced changes in the antioxidant metabolism Ajmalicine production in *Catharanthus roseus* (L.), G. Don. *Plant Sci.* **2007**, *171*, 271–276. [CrossRef]
20. Costa, M.M.; Hilliou, F.; Duarte, P.; Pereira, L.G.; Almeida, I.; Leech, M.; Memelink, J.; Barceló, A.R.; Sottomayor, M. Molecular cloning and characterization of a vacuolar class III peroxidase involved in the metabolism of anticancer alkaloids in *Catharanthus roseus*. *Plant Physiol.* **2007**, *146*, 403–417. [CrossRef]
21. Gupta, M.; Tomar, R.S.; Kaushik, S.; Mishra, R.K.; Sharma, D. Effective antimicrobial activity of green zno nano particles of *Catharanthus roseus*. *Front. Microbiol.* **2018**, *9*, 2030. [CrossRef] [PubMed]
22. Azeez, L.; Lateef, A.; Adebisi, S.A. Silver nanoparticles (agnps) biosynthesized using pod extract of cola nitida enhances antioxidant activity and phytochemical composition of *Amaranthus caudatus* Linn. *Appl. Nanosci.* **2017**, *7*, 59–66. [CrossRef]
23. Bedlovičová, Z.; Strapáč, I.; Baláž, M.; Salayová, A. A brief overview on antioxidant activity determination of silver nanoparticles. *Molecules* **2020**, *25*, 3191. [CrossRef] [PubMed]
24. Nandhini, N.T.; Rajeshkumar, S.; Mythili, S. The possible mechanism of eco-friendly synthesized nanoparticles on hazardous dyes degradation. *Biocatal. Agric. Biotechnol.* **2019**, *19*, 101138. [CrossRef]
25. Vidhu, V.K.; Philip, D. Catalytic degradation of organic dyes using biosynthesized silver nanoparticles. *Micron* **2014**, *56*, 54–62. [CrossRef]
26. Brown, M.A.; De Vito, S.C. Predicting azo dye toxicity. *Crit. Rev. Environ. Sci. Technol.* **1993**, *23*, 249–324. [CrossRef]
27. Ajmal, A.; Majeed, I.; Malik, R.N.; Idriss, H.; Nadeem, M.A. Principles and mechanisms of photocatalytic dye degradation on tio2based photocatalysts: A comparative overview. *Rsc. Adv.* **2014**, *4*, 37003–37026. [CrossRef]
28. Park, S.; Cha, S.H.; Cho, I.; Park, S.; Park, Y.; Cho, S.; Park, Y. Antibacterial nanocarriers of resveratrol with gold and silver nanoparticles. *Mater. Sci. Eng. C Mater. Biol. Appl.* **2016**, *58*, 1160–1169. [CrossRef]

29. Chand Mali, S.; Raj, S.; Trivedi, R. Biosynthesis of copper oxide nanoparticles using *Enicostemma axillare* (Lam.) leaf extract. *Biochem. Biophys. Rep.* **2019**, *20*, 100699. [CrossRef]
30. Sankar, R.; Manikandan, P.; Malarvizhi, V.; Fathima, T.; Shivashangari, K.S.; Ravikumar, V. Green synthesis of colloidal copper oxide nanoparticles using *Carica papaya* and its application in photocatalytic dye degradation. *Spectrochim. Acta A* **2014**, *121*, 746–750. [CrossRef]
31. Alam, M.W.; Al Qahtani, H.S.; Souayeh, B.; Ahmed, W.; Albalawi, H.; Farhan, M.; Abuzir, A.; Naeem, S. Novel Copper-Zinc-Manganese Ternary Metal Oxide Nanocomposite as Heterogeneous Catalyst for Glucose Sensor and Antibacterial Activity. *Antioxidants* **2022**, *11*, 1064. [CrossRef]
32. Vanaja, A.; Suresh, M.; Jeevanandam, J.; Gousia, S.; Pavan, D.; Balaji, D.; Murthy, N.B. Copper-Doped Zinc Oxide Nanoparticles for the Fabrication of white LEDs. *Prot. Met. Phys. Chem. Surf.* **2019**, *55*, 481–486. [CrossRef]
33. Behravan, M.; Hossein Panahi, A.; Naghizadeh, A.; Ziaee, M.; Mahdavi, R.; Mirzapour, A. Facile green synthesis of silver nanoparticles using *Berberis vulgaris* leaf and root aqueous extract and its antibacterial activity. *Int. J. Bio. Macromol.* **2019**, *124*, 148–154. [CrossRef] [PubMed]
34. Njagi, E.C.; Huang, H.; Stafford, L.; Genuino, H.; Galindo, H.M.; Collins, J.B.; Hoag, G.E.; Suib, S.L. Biosynthesis of iron and silver nanoparticles at room temperature using aqueous sorghum bran extracts. *Langmuir* **2010**, *27*, 264–271. [CrossRef] [PubMed]
35. Patil, S.S.; Patil, R.H.; Kale, S.B.; Tamboli, M.S.; Ambekar, J.D.; Gade, W.N.; Kolekar, S.S.; Kale, B.B. Nanostructured microspheres of silver @ zinc oxide: An excellent impeder of bacterial growth and biofilm. *J. Nanopart. Res.* **2014**, *16*, 2717. [CrossRef]
36. Kalaiselvi, A.; Roopan, S.M.; Madhumitha, G.; Ramalingam, C.; Elango, G. Synthesis and characterization of palladium nanoparticles using Catharanthus roseus leaf extract and its application in the photo-catalytic degradation. *Spectrochim. Acta Part A Mol. Biomol. Spectrosc.* **2015**, *135*, 116–119. [CrossRef] [PubMed]
37. Poopathi, S.; De Britto, L.J.; Praba, V.L.; Mani, C.; Praveen, M. Synthesis of silver nanoparticles from *Azadirachta indica*—A most effective method for mosquito control. *Environ. Sci. Pollut. Res.* **2015**, *22*, 2956–2963. [CrossRef] [PubMed]
38. Zahir, A.A.; Chauhan, I.S.; Bagavan, A.; Kamaraj, C.; Elango, G.; Shankar, J.; Arjaria, N.; Roopan, S.M.; Rahuman, A.A.; Singh, N. Green Synthesis of Silver and Titanium Dioxide Nanoparticles Using *Euphorbia prostrata* Extract Shows Shift from Apoptosis to G0/G1 Arrest followed by Necrotic Cell Death in *Leishmania donovani*. *Antimicrob. Agents Chemother.* **2015**, *59*, 4782–4799. [CrossRef]
39. Nasrollahzadeh, M.; Sajadi, S.M. Green synthesis of copper nanoparticles using *Ginkgo biloba* L. leaf extract and their catalytic activity for the Huisgen [3+2] cycloaddition of azides and alkynes at room temperature. *J. Colloid. Interface Sci.* **2015**, *457*, 141–147. [CrossRef]
40. Coury, C.; Dillner, A.M. A method to quantify organic functional groups and inorganic compounds in ambient aerosols using attenuated total reflectance FTIR spectroscopy and multivariate chemometric techniques. *Atmos. Environ.* **2008**, *42*, 5923–5932. [CrossRef]
41. Barrales-Cureño, H.J.; Montiel-Montoya, J.; Espinoza-Pérez, J.; Cortez-Ruiz, J.A.; Lucho-Constantino, G.G.; Zaragoza-Martínez, F.; Salazar-Magallón, J.A.; Reyes, C.; Lorenzo-Laureano, J.; López-Valdez, L.G. Metabolomics and fluxomics studies in the medicinal plant *Catharanthus roseus*. In *Medicinal and Aromatic Plants*; Academic Press: Cambridge, MA, USA, 2021; pp. 61–86. [CrossRef]
42. Kokila, T.; Ramesh, P.S.; Geetha, D. Biosynthesis of silver nanoparticles from Cavendish banana peel extract and its antibacterial and free radical scavenging assay: A novel biological approach. *Appl. Nanosci.* **2015**, *5*, 911–920. [CrossRef]
43. Sudha, A.; Jeyakanthan, J.; Srinivasan, P. Green synthesis of silver nanoparticles using *Lippia nodiflora* aerial extract and evaluation of their antioxidant, antibacterial and cytotoxic effects. *Resour.-Effic. Technol.* **2017**, *3*, 506–515. [CrossRef]
44. Keijok, W.J.; Pereira, R.H.A.; Alvarez, L.A.C.; Prado, A.R.; da Silva, A.R.; Ribeiro, J.; Guimarães, M.C.C. Controlled biosynthesis of gold nanoparticles with Coffea arabica using factorial design. *Sci. Rep.* **2019**, *9*, 16019. [CrossRef]
45. Murali, M.; Mahendra, C.; Rajashekar, N.; Sudarshana, M.S.; Raveesha, K.A.; Amruthesh, K.N. Antibacterial and antioxidant properties of biosynthesized zinc oxide nanoparticles from *Ceropegia candelabrum* L.—An endemic species. *Spectrochim Acta A Mol. Biomol. Spectrosc.* **2017**, *179*, 104–109. [CrossRef]
46. Supraja, N.; Prasad, T.N.; Krishna, T.G.; David, E. Synthesis, characterization, and evaluation of the antimicrobial efficacy of *Boswellia ovalifoliolata* stem bark-extract-mediated zinc oxide nanoparticles. *Appl. Nanosci.* **2015**, *6*, 581–590. [CrossRef]
47. Wu, S.; Rajeshkumar, S.; Madasamy, M.; Mahendran, V. Green synthesis of copper nanoparticles using *Cissus vitiginea* and its antioxidant and antibacterial activity against urinary tract infection pathogens. *Artif. Cells Nanomed. Biotechnol.* **2020**, *48*, 1153–1158. [CrossRef] [PubMed]
48. Ferreres, F.; Pereira, D.M.; Valentão, P.; Andrade, P.B.; Seabra, R.M.; Sottomayor, M. New phenolic compounds and antioxidant potential of *Catharanthus roseus*. *J. Agric. Food Chem.* **2008**, *56*, 9967–9974. [CrossRef]
49. Dobrucka, R. Facile synthesis of trimetallic nanoparticles au/cuo/zno using vitex agnus-castusextract and their activity in degradation of organic dyes. *Int. J. Environ. Anal. Chem.* **2019**, *101*, 2046–2057. [CrossRef]
50. Liu, C.; Li, Y.; Chen, Y.; Liang, Y.; Liu, S.; Guo, H. Biosynthesis of silver nanoparticles by garlic extract and their antioxidant activity. *J. Nanosci. Nanotechnol.* **2017**, *17*, 5964–5971.
51. Rizwan, M.; Yahya, R.; Khatoon, A.; Shaari, A. Green synthesis of trimetallic gold-silver-copper nanoparticles and their potential as antioxidant agents. *J. Inorg. Organomet. P* **2019**, *29*, 877–883.
52. Mittal, A.; Jhare, D.; Mittal, J. Adsorption of hazardous dye Eosin Yellow from aqueous solution onto waste material De-oiled Soya: Isotherm, kinetics and bulk removal. *J. Mol. Liq.* **2013**, *179*, 133–140. [CrossRef]

53. Yuan, M.; Fu, X.; Yu, J.; Xu, Y.; Huang, J.; Li, Q.; Sun, D. Green synthesized iron nanoparticles as highly efficient fenton-like catalyst for degradation of dyes. *Chemosphere* **2020**, *261*, 127618. [CrossRef] [PubMed]
54. Li, H.; Wang, L.; Zhang, Y.; Liu, Q.; Sun, Z. Trimetallic Fe-Pd-Cu nanoparticles for enhanced catalytic degradation of eosin yellow. *J. Nanopart Res.* **2019**, *21*, 1–11.
55. Liu, Y.; Li, J.; Yang, H.; Sun, S. Degradation of eosin yellow by bimetallic Fe/Ni nanoparticles: Optimization, kinetics and mechanisms. *J. Hazard Mater.* **2021**, *416*, 125874.